DESIGN AND CONSTRUCTION OF CW DYE LASER

Karl-Heinz Friedrich Kelle

NAVAL POSTGRADUATE SCHOOL
Monterey, California

THESIS

DESIGN AND CONSTRUCTION OF A CW DYE LASER

Karl-Heinz Friedrich Kelle

Thesis Advisor: John P. Powers

June 1972

Design and Construction of a CW Dye Laser

by

Karl-Heinz Friedrich Kelle
Lieutenant, Federal German Navy

Submitted in partial fulfillment of the
requirements for the degree of

MASTER OF SCIENCE IN ELECTRICAL ENGINEERING

from the
NAVAL POSTGRADUATE SCHOOL
June 1972

ABSTRACT

The properties of organic dyes as well as the lasing process of organic dye lasers are investigated to form the basis for the design of a cw dye laser. Different dye laser systems are compared with regard to stability, utility, and construction characteristics. A folded three mirror resonator with an inserted dye cell set at the Brewster angle is chosen and analysed. The astigmatic effects introduced by the tilted mirror can be offset by those from the dye cell to yield a compensated cavity. The trade-offs and limitations given by the cell thickness, the angle of incidence, and the focal length of the center mirror are discussed. Finally, experimental data and procedures are given.

ACKNOWLEDGMENT

I am very grateful for the help and support given by Professor John P. Powers of the Naval Postgraduate School and Mr. A. Dienes of the Bell Telephone Laboratories. I want to thank Mrs. Deloris J. Robinson for the final typing, Mr. Robert C. Scheile for the Construction of the dye cell and Mr. Michael O'Dea for building the cell and mirror mounts.

TABLE OF CONTENTS

I. INTRODUCTION

When in 1960 Maiman [1] presented the first optical maser and Sorokin and Stevenson [2] obtained situmlated emission in a four-level laser system (systems as explained by Yariv and Gordon [3]), the ground was broken for a vast variety of laboratory work and prediction in the field of lasers.

It seemed to be no surprise when the well known process of luminescence in organic materials was among the early suggestions for the laser operation. In 1961 Brock et. al. [4] and, independently Rautian and Sobelman [5] theoretically considered phosphorescence lasing and their results seemed to be verified by the experimental results given by Morantz et. al. [6]. But the results of these investigations were questioned [7]. Subsequently this approach to obtaining laser action was dropped.

Stockman et. al. [8] recognized the advantages of a fluorescent emission over a phosphorescent one for lasing, but they were not able to get any experimental verification of their ideas (although they were correct). Experimental success came with the work of Sorokin and Lankard [9]. This system, with the lasing medium excited by a giant-pulse ruby laser, is considered to be the first true optically pumped organic laser (if one sets aside the lasers based on the rare-earth chelates).

The same two authors achieved organic dye laser action by flashlamp excitation in 1967 [10].

The report of CW-operation of an organic dye laser by Peterson et. al. [11] was another major step in this part of the laser field, which is very promising for the following reasons:

(a) Dyes, usable for laser operation, are available over the entire visible spectrum and beyond; typical values ~3400- 11,750 Å.

(b) Dye lasers are continuously tunable; ranges of over 1700 Å have been obtained [12].

(c) The spectral width of the normally broad band emission can be narrowed to single Angstroms; minimum values of less than 0.01 Å have been obtained [13].

(d) Conversion efficiencies of nearly 30% have been obtained in laser pumped organic dye lasers [14].

II. PROPERTIES OF ORGANIC DYES

A. DYE CHEMISTRY

This section summarizes material presented in Ref. [15]:

(1) A strong fluorescence is an essential prerequisite for the lasing action of an organic dye laser. This property determines some specific dye families for laser operation:

- Oxazole
- Xanthene
- Anthracene
- Coumarin
- Acridine
- Azine
- Phthalocyanine
- Polymethine

See TABLE I for further specifications of some typical dyes of these families.

(2) Reports indicated that the number of dyes which lase under excitation of another laser is greater than those that are excited by flashlamps. Most dyes that could be flashlamp excited belong to the Xanthenes and the Coumarins.

(3) Chemical or photochemical instability can be a major problem for dyes, especially if their decomposition products absorb at the wavelength of the emission.

(4) The Xanthenes seem to be the most promising dyes because lasing action is most easily achieved and they absorb and emit light

TABLE I [15 , 17]
Chemical Structure and Data for Typical Laser Dyes

Family	Chemical Structure/Name	Molecular Weight	Chemical formula
Oxazole	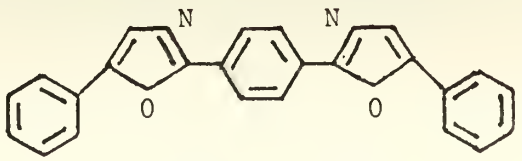 or p-Bis[2-(5-phenyloxazolyl)]benzene	364.40	$C_{24}H_{16}N_2O_2$
Xanthene	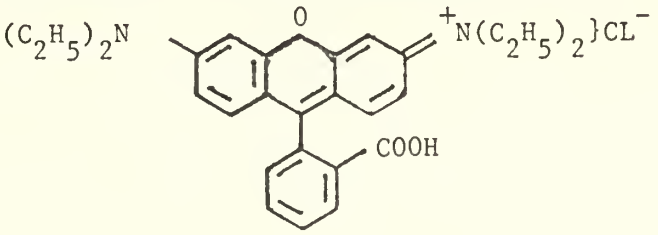 Rhodamine B	479.02	$C_{28}H_{31}ClN_2O_3$
Xanthene	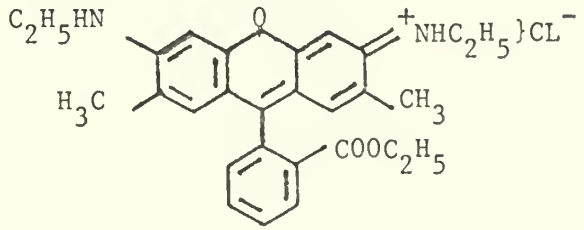 Rhodamine 6G	479.02	$C_{28}H_{31}ClN_2O_3$
Acridine	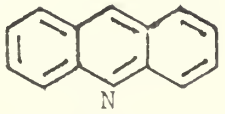 Acridine	179.22	$C_{13}H_9N$

Family	Chemical Structure/Name	Molecular weight	Chemical formula
Anthracene	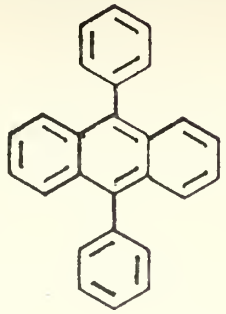 9, 10-Diphenylanthracene	330.43	$C_{26}H_{18}$
Coumarin	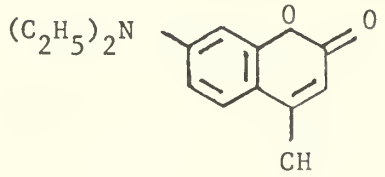	231.30	$C_{14}H_{17}NO_2$
Polymethine	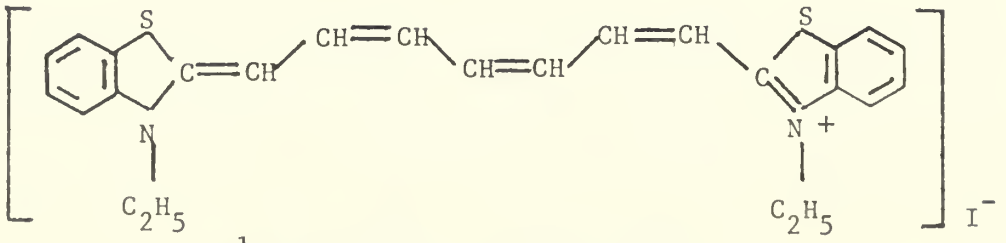 $3,3^1$-Diethylthiatricarbocyanineiodide		

chiefly in the visible part of the spectrum. Also they are more stable under visible and UV-radiation than Polymethines.

(5) Oxazoles, Coumarins, and Anthracenes mostly absorb in the near UV and emit in the violet or blue region of the spectrum.

B. SPECTROSCOPY

Reference [15] gives a very useful general summary of the spectral properties of organic dyes as well as further references. The summarizing statements are restated here:

(1) The widths of the principal absorption and emission bands of these dyes are generally on the order of $1000cm^{-1}$. One or more absorption bands may be found towards the UV from the principal absorption.

(2) The fluorescence peak occurs at longer wave lengths than the principal absorption peak..... The extent of this Stokes shift and the width of the fluorescence and absorption spectra may be such that the short wavelength tail of the fluorescence substantially overlaps the long wavelength tail of the absorption.

(3) The fluorescence spectrum is generally a mirror image of that of the principal absorption band (Figure 1).

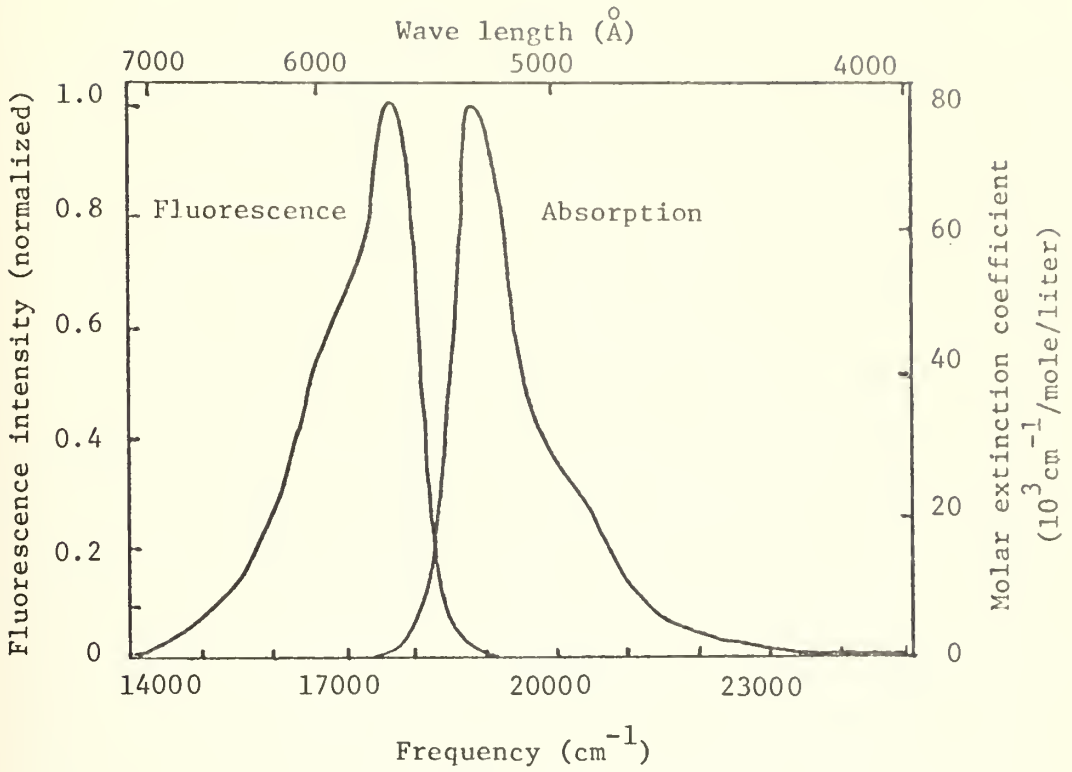

Fig. 1: Absorption and fluorescence spectra of 10^{-4}M rhodamine 6G in ethanol [18]

(4) The fluorescent lifetime is typically 5×10^{-9} sec.

(5) Excited - triplet absorption band may overlap the fluorescence band and may persist for as long as 10^{-3} sec, depending on the solution treatment (Figure 2).

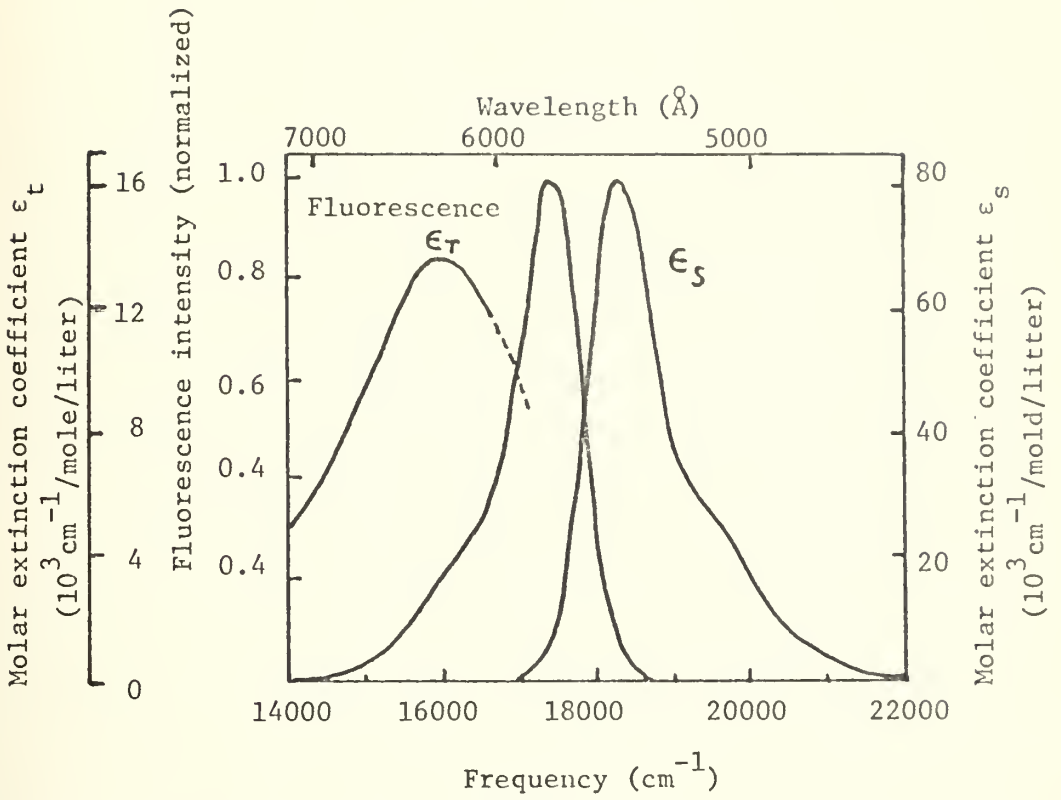

Fig. 2: Singlet absorption and fluorescence spectra of 5 x 10^{-5}M rhodamine B in methanol and triplet-triplet absorption absorption spectrum in polymethylmethacrylate [18].

C. ENERGY LEVEL CONSIDERATIONS

1. Basic Energy Level Structure

General laser operation of any kind is best understood by considering the physical interaction in the atoms or molecules of the laser material with the help of an energy level diagram. All molecules exhibit electronic spectra (due to the change in the electronic configuration of the molecule) with rotational and vibrational fine structures (due to the motion of the molecule's atomic nuclei). These energy level diagrams are relatively easy to represent for atomic or simple molecular gas lasers and solid-state lasers but are extremely complicated for the large, complex dye molecules.

In order to preserve a helpful tool while avoiding too much complexity, it is generally accepted that one can represent the energy level diagram for a dye molecule by using the theory of a diatomic molecule (which is similar to the quantum mechanical harmonic oscillator problem). The potential energy of the diatomic molecule is plotted as a function of a single variable, the internuclear distance, R. The different energy levels can now be calculated by consideration of the various selection rules. Typical separations of energy levels are given by:

electronic - electronic:	several electron volts
vibrational - vibrational:	0.1 eV
rotational - rotational:	10^{-3} eV

Due to the very small energy separation between rotational levels they appear as a continuum on a normal energy scale and are neglected in the following figures.

Figure 3 contains curves of potential energy versus internuclear distance for the electronic ground state and first excited state in a diatomic molecule as well as the vibrational energy levels of each state. Superimposed on the vibrational energy levels are graphs of the corresponding harmonic-oscillator probability densities (i.e. evaluation of $|\Psi|^2$, where Ψ is defined as the wave function). The densities indicate the likelihood that the nuclei of the diatomic molecule will be a specific distance, R, apart.

Assuming that electronic and vibrational transitions are so rapid that instantaneous internuclear distances remain fixed while they occur (Franck-Condon principle [16]), transitions must be indicated by vertical lines on the energy level diagram. Transitions are favored that occur between positions with highest probability densities in two different energy levels.

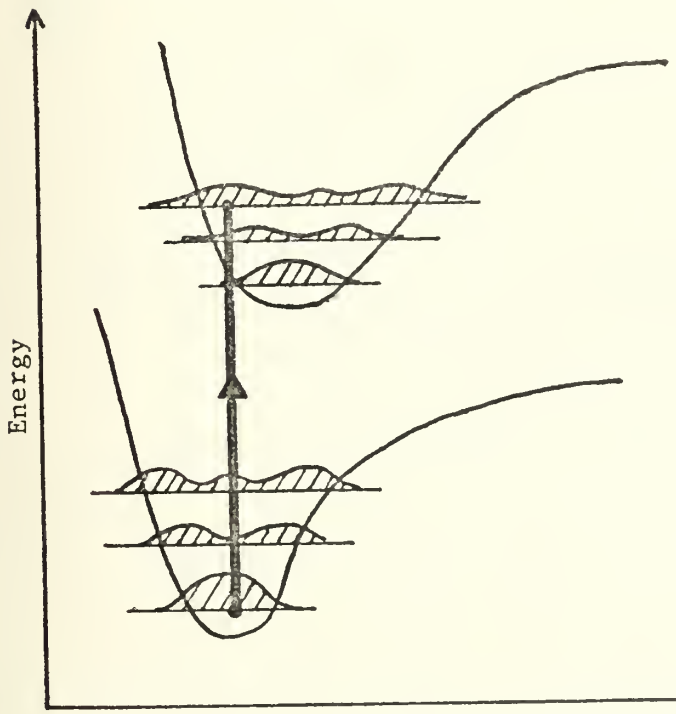

Fig. 3: Vibrational energy levels and associated probability densities for two electronic states of a diatomic molecule. The vertical line indicates an electronic transition.

Prior to consideration of the laser process one has to make one further assumption. For the diatomic model it is possible to assume that the configuration of states can be described by only one variable, although a dye molecule's potential energy generally is a function of more than one variable.

2. Basic Dye Laser Process

The laser process based on the fluorescent radiation of the dye can now be explained (Figure 4) as interaction between two singlet-states, S_o (electronic energy level, ground state) and S_1, (electronic energy level, first excited state):

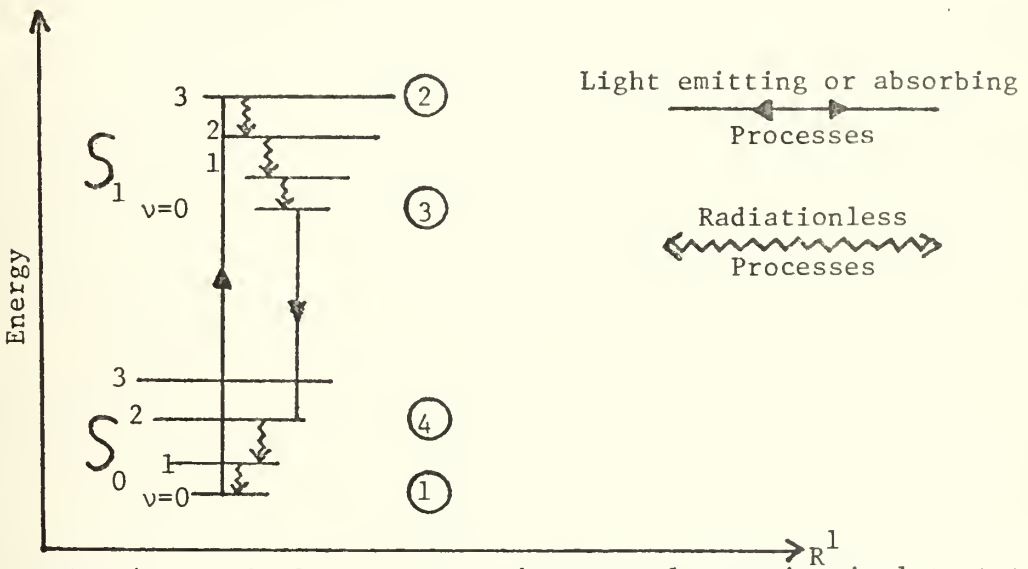

Fig. 4: Basic laser process between electronic singlet-states. Principal laser levels are indicated 1 - 4 . $\nu \equiv$ vibarational quantum number, $\nu = 0,1,2,...$)

Optical excitation pumps the molecular electrons from the zero-point level (v=0) of the ground state, S_o (indicated as (1)), to a higher vibrational-rotational energy level in the first excited singlet-state, S_1 (indicated as (2)). By numerous collisions between molecules the single molecule loses part of its vibrational energy and drops in very rapid transitions to the zero-point level of the first excited

singlet-state, ③. These radiationless processes are called internal conversions.

In order to accomplish the laser action by stimulated emmission (fluorescent radiation) between the upper laser level, ③, and the lower one, ④, the system must reach population inversion (at least the critical inversion) between these two levels. This is attained by accumulating particles in laser level ③ and rapid depopulation of laser level ④ .

The accumulation of particles in level ③ is achieved since the decay from level ③ (which normally is taken as the fluorescent lifetime, ~5×10^{-9} sec) is much slower, at least by a factor of 10^3[19], than the internal conversion, ② → ③. The rapid depopulation of the lower laser level ④ by radiationless transition to level ① is governed by the same small internal conversion time factor as the ②→③transition.

The process described above indicates a four-level laser system. Experimental verification of this model is given by Ref. [18] and Ref. [20]. Both show that the relative population (for critical inversion), n_{SC}, of level ③ is less than one half, where the relative population is defined by:

$$n_{SC} \equiv \frac{N_{S1}}{N}$$

where N_{S1} = density of molecules in level ③

N = total density of molecules in system

The experimental values of Ref. [20] are partly restated in TABLE II.

TABLE II

Critical Inversion and Triplet-State Concentration for Laser Dyes at the Onset of Oscillation (Flashlamp excited)

Dye and Solvent	N_{S1} (10^{15} cm^{-3})	N_{S1}^* (10^{15} cm^{-3})	N_t (10^{15} cm^{-3})	N_t (%)	N_{S1}^*/N_{S1}	λ_1 (nm)
Rhodamine B						
10^{-4}M, methanol	0.039	0.93	5.5	8.4[1]	23.8	615
Rhodamine 6G						
10^{-4}M, ethanol	0.214	0.84	2.9	4.4[1]	3.9	579

There are major effects due to triplet-states, which have not been considered up to now, in the overall performance of the system. The general lasing process as described above remains valid but it is more difficult to reach the critical inversion. This is based on the fact that the upper laser level is not only depopulated by fluorescence but also by non-radiative transitions between the singlet and the triplet-state (intersystem crossing). The above considerations are indicated by the discrepancy between N_{S1} and N_{S1}^* as shown in TABLE II.

Since the ground state is a single-state, the intermediate state between the ground state and the first excited singlet-state is a (at least one) triplet-state because of selection rules.

---

[1] The evaluation of N_t (%) seems to result in slightly different numbers:

1 M solution contains 6.023×10^{23} molecules/liter

10^{-4} M solution contains 6.023×10^{16} molecules/cm^3

Rhodamine B: $\frac{N_t}{6.023 \times 10^{16}} \times 100 = 9.1\ \%$

Rhodamine 6G: $\frac{N_t}{6.023 \times 10^{16}} \times 100 = 4.8\ \%$

where 6.023×10^{23} mole^{-1} is Avogadro's number.

Singlet-triplet (S-T) transitions do occur but at a much lesser rate than "spin-allowed" transitions between singlet-singlet (S-S) or triplet-triplet (T-T) states. These S-T transitions are called "spin-forbidden". A more complete energy level diagram is given in Figure 5. This diagram includes triplet-states.

To complete one's understanding of the lasing process the following explanations have to be added:

The zero-point level of the first triplet-state, T_1, is a mestastable (lifetime under normal conditions 10^{-3} sec) level and acts as a particle trap. It not only depopulates the upper laser level, (3), but it deprives the lasing system of the necessary molecules to reach the critical inversion. The depopulation can prevent any laser action if the S-S absorption ((1) → (2)) is too slow to reach the critical inversion. The extraction of particles can stop the laser action, if the density of the molecules in the zero-point ground state, (1) , is so small that one can not preserve the critical inversion.

Another drawback for the lasing operation is the T-T absorption, which takes place at a longer wavelength than the principal S-S absorption (Figure 5). This T-T absorption might therefore compete directly with the lasing action, S-S emission, since their wavelengths can overlap (Figure 2).

The S_1-S_2 absorption is very weak, because of the small population density of the first excited singlet-state, S_1.

3. Intersystem Crossing

Although a complete understanding of intersystem crossing is not necessary to explain lasing phenomena a simple description might help to complete the picture. Three different energy level situations

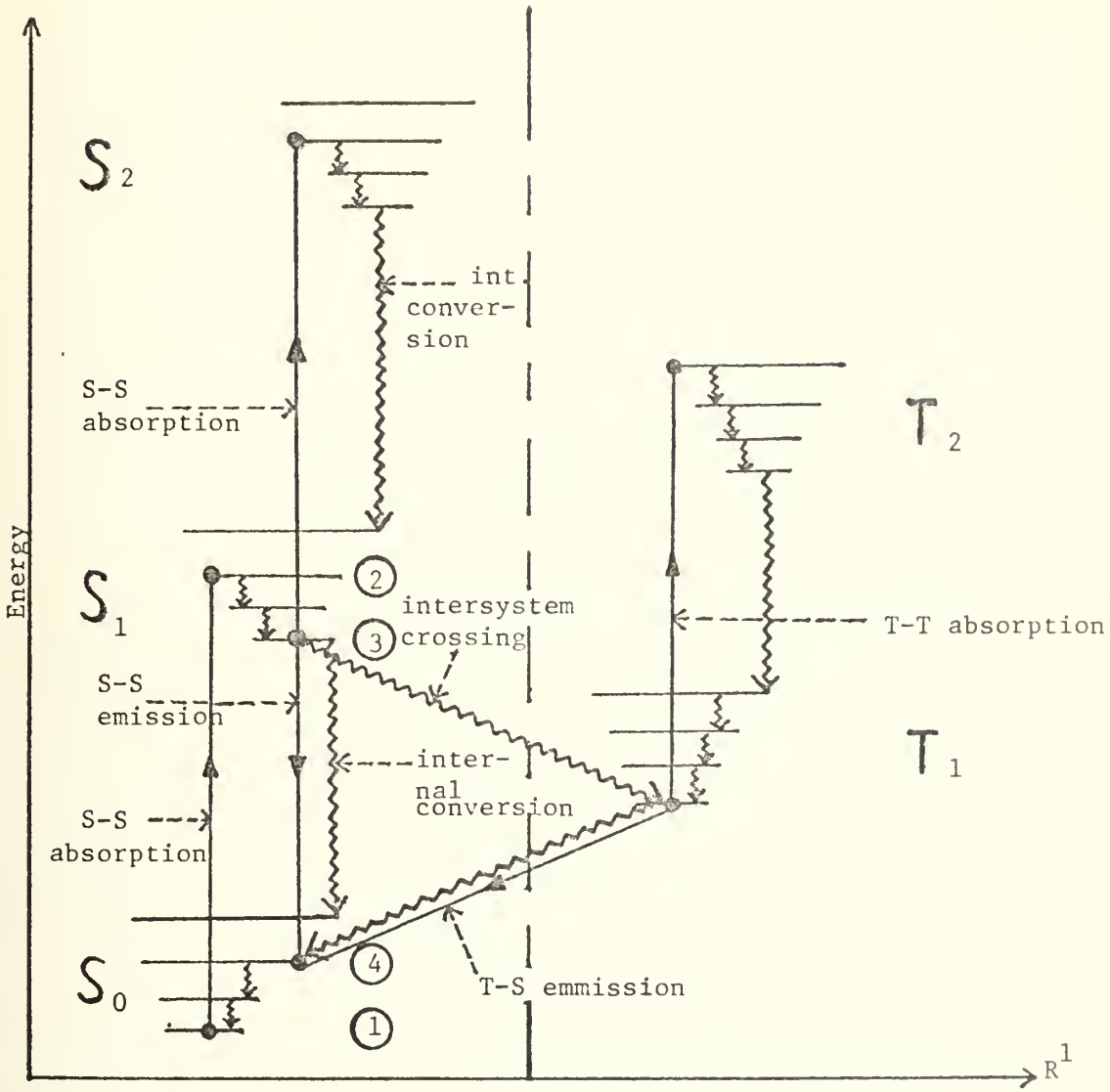

Fig. 5: Schematic energy level diagram for a dye molecule including significant electronic and vibrational transitions. (For clarity the origin of the triplet-states is shifted to the right on the R^1 coordinate).

are discussed briefly. For all these situations one assumes that the population density of the higher vibrational levels of the first excited singlet-state is very small in comparison to the zero-point level of that state.

(1) (Figure 6a): The only form of intersystem crossing expected is that from the zero-point level of S_1 to the zero-point level of T_1. This is the situation described previously.

(2) (Figure 6b): The energy levels of S_1 and T_1 are so close together that one can expect a nearly perfect energy match between a vibrational level of S_1 and one of T_1. In this case there might be a different path for the intersystem crossing as one could expect a significant contribution form the vibrational levels, since their energy gap is so small.

(3) (Figure 6c): In this configuration it seems not very possible that a direct intersystem crossing occurs between S_1 and T_1, since the energy gap is too large for that kind of spin-forbidden transition. One might expect, with a higher probability, an intersystem crossing between S_1 and T_2, similar to that described in (2), followed by a spin-allowed internal conversion between T_2 and T_1.

Most of the above, mainly in (2) and (3), are predictions of intersystem crossing which have not been verified experimentally. Some attempts are given by References [19], [21] , [22].

For the purpose of understanding the dye laser process, one can assume that the internal conversion is so rapid that most of the intersystem crossing occurs from the zero-point level of the first excited singlet-state to the zero-point level of the first triplet-state, governed by the rate constant K_{ST}, where $K_{ST} \sim 10^{-8}$ sec^{-1}.

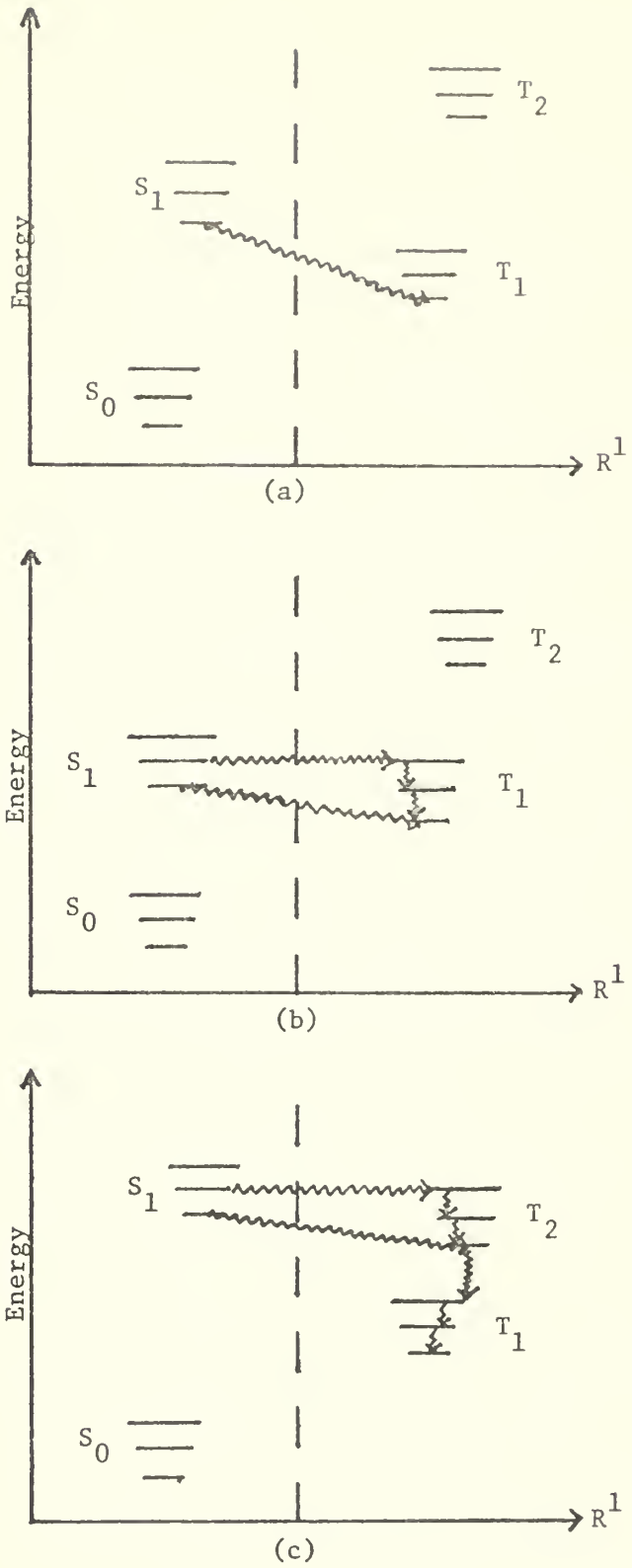

Fig. 6: Intersystem crossing considered under three different energy level situations

4. Summary of Properties of Organic Dyes

The purpose of this summary is to state facts or considerations which are fundamental for the design of a CW dye laser.

(1) Rhodamine 6G seems to be the most promising organic dye for the following reasons:

- it emits and absorbs in the visible spectrum (absorption spectrum can be matched with the output of an Argon laser)
- it produces the greatest efficiencies and highest output powers
- it is stable when optically pumped

(2) To achieve and to maintain the critical inversion for a CW operation one needs a high power (laser) pumping source.

(3) In order not to destroy the dye by the optical pumping process the dye must be circulated rapidly.

(4) The lifetime of the molecules in the metastable (10^{-3} sec) triplet-state must be decreased to achieve CW lasing. This is called triplet quenching.

III. DESIGN OF A CW DYE LASER

A. LITERATURE SURVEY AND GENERAL CONSIDERATIONS

Despite the fact that triplet quenchers were known for a long time the major breakthrough towards the CW operation of the dye laser was achieved by the long-pulse experiments of Snavely and Schäfer [23]. They were able to decrease the triplet lifetime of rhodamine 6G to about 10^{-7} sec but failed to experimentally obtain CW operation because of the problem of optical inhomogeneities in the active medium (introduced by temperature gradiants due to the high intensity of the optical pumping).

Peterson et. al. [11] overcame that problem by using an active medium whose index of refraction was only slightly temperature dependent (a water solution instead of a methanol one) and a dye cell with windows of high thermal conductivity (sapphire instead of quartz or pyrex). They achieved the first CW dye laser operation, with a longitudinally, externally excited laser system.

These systems, discussed by Tuccio and Strome [24], are based on the following considerations:

The threshold conditions (assuming a required pumping power density of 100 KW/cm^2 with 2% cavity losses and a triplet lifetime of $\sim 10^{-7}$ sec) must be fulfilled continuously. That was not possible with flashlamp excitation but were possible, for example, with argon lasers with a single line output of 1 Watt and a beam diameter of 2mm at the $1/e^2$ intensity points.

In order to exceed the threshold by a factor of three to ten, one has to focus this excitation laser beam to a spot diameter between 20 and 10 μm.

To utilize the maximal pump power one has to match the pump beam diameter very accurately with the diameter of the dye lasing mode (Perterson et. al. [11] indicated the match of a 11μm pump beam with a 12μm lasing mode). These circumstances made the critical alignement of excitation source and laser cavity necessary.

Tuccio and Strome [24] present a Two-Element and a Three-Element cavity design.

The Two-Element system (Figure 7a) shows very sensitive relationship between lasing mode spot size and mirror spacing. One can decrease the sensitivity of the system by decreasing the cavity length, which naturally reduces the utility of the system, e. g. one cannot insert tuning or modulating elements.

The contradiction of long cavity length and small spot size is solved by a Three-Element system. In such a system, more often called a resonator with internal lens (Figure 7b), the spot size depends on the focal length of the lens and not on the mirror spacing.

Thermal effects associated with both of these externally pumped cavities introduced severe limitaitons to the laser operation. The energy transfer spot (excitation → lasing) is located immediately inside the entrance window of the dye cell. Without a window material of high heat conductivity it was impossible to reach laser operation [11]. This small, hot spot is able to damage the coating on the mirror as well as the dye unless the dye is circulated rapidly. A high flow rate and a temperature insensitive dye solvent can compensate for these

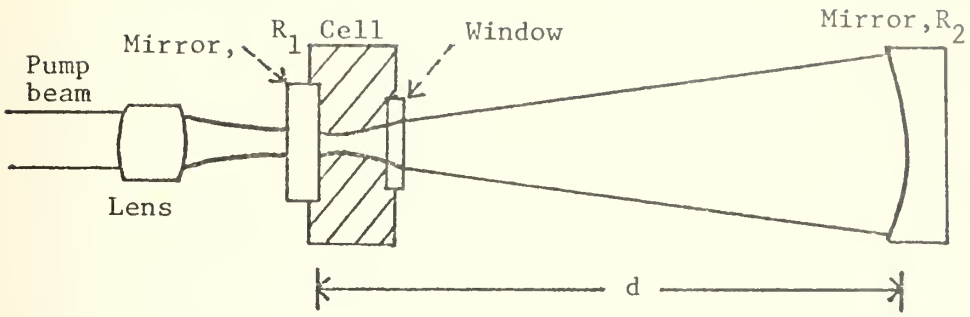

Fig. 7a: Two Element cavity. R_2 and d are approximately equal. [24]

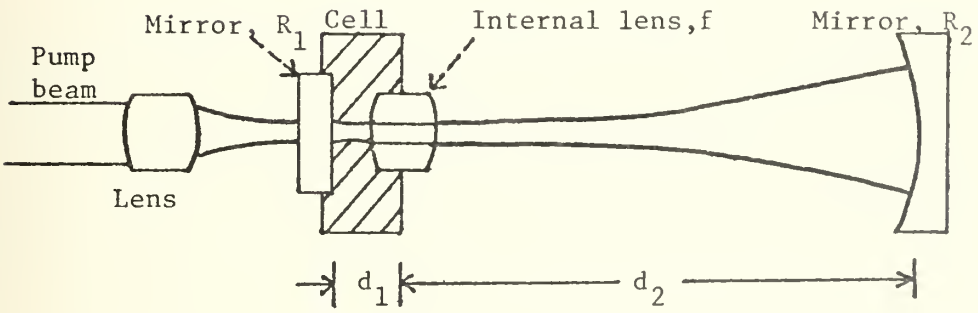

Fig. 7b: Three Element cavity with an internal lens. Mirror R_1 is approximately at the focal point of the lens. [24]

thermal effects. When the input power density exceeds 1 MW/cm^2 output losses are still quite evident [24], even with high flow rates.

A modified version of the Three-Element system is the folded cavity, used for example with an acoustooptic modulator by Maydan [25]. The folded cavity preserves the long cavity - small focus advantages in addition to decreasing any optical losses introduced by the inserted lens in the Three Element system. Kohn et. al. [26] inserted the dye cell at the focal point of the folded cavity (Figure 8), and were able to operate the system continuously. This system, which now is internally pumped, has several advantages over the externally pumped one:

(1) The dye laser is automatically aligned with the excitation laser, since both lase in the same cavity.

(2) The power coupling into the dye occurs from the standing wave of the excitation laser, i.e. the heat is generated nearly uniformly along the pumping axis. This avoids forming the hot spot.

(3) The thermally induced inhomogeneities can be compensated by cavity adjustments.

The disadvantages of the folded cavity are easily recognized. Both the tilted mirror and the inserted dye cell which is usually at the Brewster angle to minimize reflections introduce astigmatic effects, that are detrimental to the required tight focus. It is assumed that the astigmatism dominates any other optical aberration.

The design task is to offset the astigmatic effects of the mirror with those of the Brewster cell to gain a compensated cavity [26], i. e. find a relation between the angle of incidence θ and the cell thickness t (Figure 8) to achieve compensation.

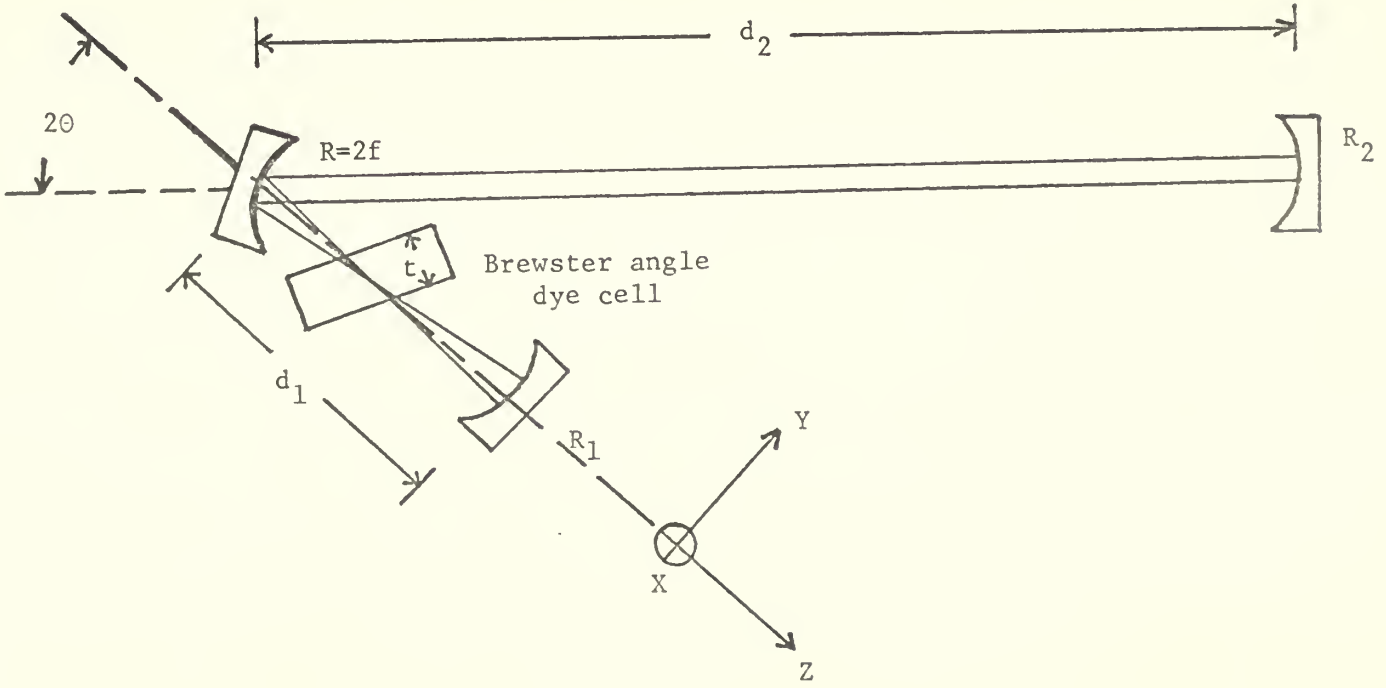

Fig. 8: Folded cavity with inserted Brewster angle dye cell

B. STABILITY CONSIDERATIONS FOR A RESONATOR WITH INTERNAL LENS

Kogelnik [27] showed in his analysis of resonators with internal lenses, that a system such as in Figure 9a could be replaced by an equivalent empty resonator system as in Figure 9b.

The following summarizes Kogelnik's analysis, as pertinent to the present problem.

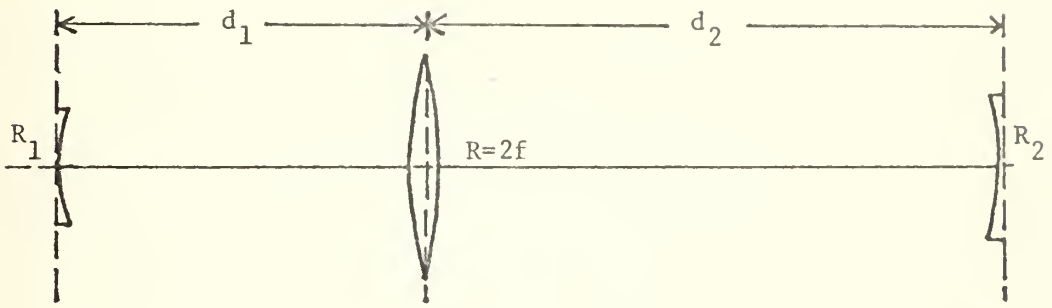

Fig. 9a: Resonator with internal lens [27]

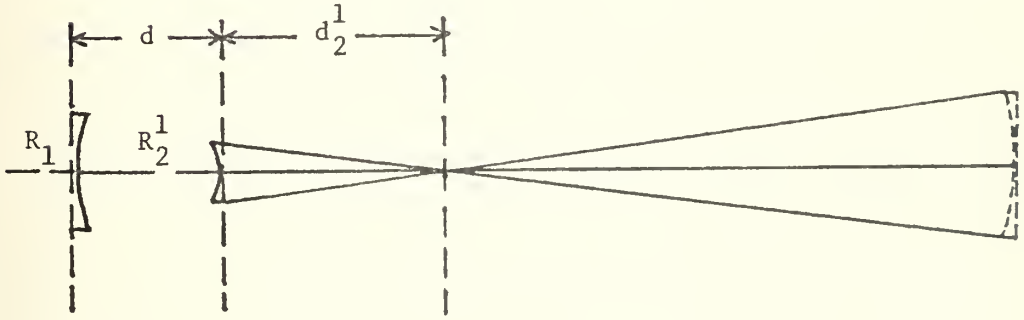

Fig. 9b: Equivalent empty resonator [27]

It is required that

$$d = d_1 - d_2' = d_1 - \frac{fd_2}{d_2 - f} \tag{3.1}$$

The radius of curvature of the substitute mirror (R_2^*) can be found by imaging the center of curvature of mirror R_2.

Evaluating

$$\frac{1}{f} = \frac{1}{d_2' + R_2^*} + \frac{1}{d_2 - R_2} \tag{3.2}$$

yields

$$R_2^* = \frac{R_2 f}{(d_2 - f)(d_2 - f - R_2)} \tag{3.3}$$

The stability of a resonator of this kind is given by

$$0 \leq (1 - \frac{d}{R_1})(1 - \frac{d}{R_2^*}) \leq 1 \tag{3.4}$$

which limits the mirror spacing d_1 to a small range near

$$d_1 = R_1 + f \tag{3.5}$$

This possibility of an adjustment of the mirror spacing lead Koeglnik et. al. [28] to define an adjustment measure δ by stating the spacing d_1 as

$$d_1 = R_1 + f + \delta \tag{3.6}$$

One can now define a stability range 2S as

$$2S \equiv \delta_{max} - \delta_{min} \tag{3.7}$$

where δ_{max} and δ_{min} are determined by the stability limits of Eq. 3.4. These limits are obtained when

$$d = R_1 + R_2^* \tag{3.8}$$

or

$$d = R_1 \tag{3.9}$$

δ_{max} and δ_{min} are evalusted by inserting 3.1, 3.8, 3.19 into 3.6

$$\delta_{max} = \frac{f^2}{d_2 - f - R_2} \tag{3.10}$$

$$\delta_{min} = \frac{f^2}{d_2 - f} \tag{3.11}$$

These equations yield a stability range

$$2S = - \frac{R_2 f^2}{(d_2 - f)(d_2 - f - R_2)} \tag{3.12}$$

For small spot cavities (Ref. [26]) one normally adjusts

$$d_2 >> f$$

and

$$R_2 = \infty$$

This simplifies 3.12 to approximately

$$2S \sim \frac{f^2}{d_2} \tag{3.13}$$

This estimate of the stability range will be used later in the design.

C. COMPENSATED CAVITY

1. Mirror Astigmatism

Light incident to a mirror at an oblique angle as in Figure 8 (folded cavity) is reflected to different focal positions (f_x, f_y), depending on whether it travels in the sagittal (X Z) or in the tangential (Y Z) plane (Figure 8). Gauss' thin lens equation (without astigmatism) is

$$\frac{1}{p} + \frac{1}{q} = \frac{1}{f} \tag{3.14}$$

where $p \equiv$ object distance

$q \equiv$ image distance.

This equation has to be modified [29] to

$$\frac{1}{p} + \frac{1}{q_x} = \frac{\cos\Theta}{f} \tag{3.15}$$

and

$$\frac{1}{p} + \frac{1}{q_y} = \frac{1}{f\ \cos\Theta} \tag{3.16}$$

where q_x and q_y represent the image distances in the sagittal and in the tangential plane respectively.

Hence one can define two effective focal lengths

$$f_x \equiv \frac{f}{\cos\Theta} \tag{3.17}$$

$$f_y \equiv f\ \cos\Theta \tag{3.18}$$

2. Brewster Cell Astigmatism

The astigmatic behaviour of light rays in the Brewster angle dye cell can be expressed by two effective distances, as shown by Hanna [30]:

$$d_{x\ cell} = \frac{t}{(n^2 - \sin^2\Phi_B)1/2} \tag{3.19}$$

$$d_{y\ cell} = \frac{tn^2(1 - \sin^2\Phi_B)}{(n^2 - \sin^2\Phi_B)^{3/2}} \tag{3.20}$$

where $n \equiv$ index of refraction of the dye cell (treating the cell windows and the dye as an homogeneous material). The other parameters are indicated in Figure 10.

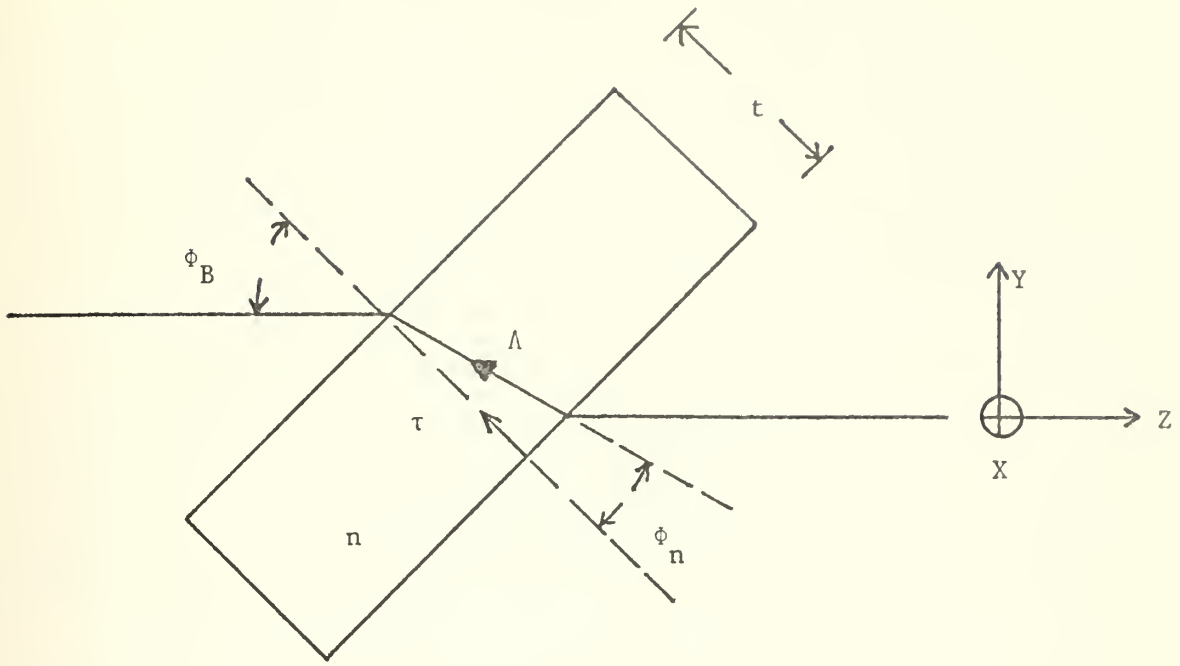

Fig. 10: Brewster angle dye cell

Using the identities

$$\sin^2 x + \cos^2 x = 1$$

and $\dfrac{\sin \Phi_B}{\cos \Phi_B} = \tan\Phi_B = n$ ($\Phi_B \equiv$ Brewster angle)

one gets

$$\sin^2\Phi_B = \frac{n^2}{n^2 + 1} \tag{3.21}$$

Inserting 3.21 into 3.19 and 3.20 yields

$$d_{x\text{ cell}} = \frac{t(n^2 + 1)^{1/2}}{n^2} \tag{3.22}$$

$$d_{y\text{ cell}} = \frac{t(n^2 + 1)^{1/2}}{n^4} \tag{3.23}$$

3. Compensation of Astigmatism

Following the procedure of section III. B. (definition of an adjustment measure) and evaluating the folded cavity using the results of sections III. C. 1. and III. C. 2., the effective mirror separation in the short leg of the cavity can be defined as:

$$d_{lx} \equiv d_{air} + d_{x\ cell} = R_1 + f_x + \delta_x \tag{3.24}$$

$$d_{ly} \equiv d_{air} + d_{y\ cell} = R_1 + f_y + \delta_y \tag{3.25}$$

In these equations d_{air} is that part of d_1 where the beam propagates in the air. This quantity is the same in the sagittal and in the tangential planes.

The quantities of the stability range, 2S (3.13), and the adjustment measures δ_{max} and δ_{min} (3.10, 3.11) are governed by the factor f^2. This factor has to be modified in accordance with the effective focal lengths f_x (3.17) and f_y (3.18) to give

$$2S_x \sim \frac{f^2}{\cos^2\Theta\, d_2} \tag{3.26}$$

$$2S_y \sim \frac{f^2 \cos^2\Theta}{d_2} \tag{3.27}$$

$$\delta_{x\ max} = \frac{f^2/\cos^2\Theta}{d_2 - f/\cos^2\Theta - R_2} \tag{3.28}$$

$$\delta_{x\ min} = \frac{f^2/\cos^2\Theta}{d_2 - f/\cos\Theta} \tag{3.29}$$

$$\delta_{y\ max} = \frac{f^2 \cos^2\Theta}{d_2 - f\cos\Theta - R_2} \tag{3.30}$$

$$\delta_{y\ min} = \frac{f^2 \cos^2\theta}{d_2 - f\cos\theta} \tag{3.31}$$

If one assumes that the angle of incidence θ does not exceed $10°$ ($\cos^2 10° = 0.97$) the value of the above parameters are shifted upwards or downwards, in the sagittal or in the tangential plane respectively, by less than 3%, which is tolerable. One can then state:

$$2S_x \sim 2S_y \sim 2S \tag{3.32}$$

$$\delta_{x\ max} \sim \delta_{y\ max} \sim \delta_{max} \tag{3.33}$$

$$\delta_{x\ min} \sim \delta_{y\ min} \sim \delta_{min} \tag{3.34}$$

But even if the limiting values of these parameters are essentially the same, the actual δ_x and δ_y are in general different. The stability ranges, $2S_x$ and $2S_y$, can be associated with different ranges of spatial positions even though they have equal values. The general idea of a compensated cavity is to produce a maximum overlap of the ranges of positions associated with $2S_x$ and $2S_y$. This would give the maximum possible compensation.

To provide the compensation one proceeds as follows: Subtracting 3.25 from 3.24 and setting the difference of the adjustment measure to zero, yields

$$d_{x\ cell} - d_{y\ cell} = f_x - f_y \tag{3.25}$$

Inserting 3.22, 3.23, 3.17, and 3.18 into 3.35 one gets

$$\frac{t(n^2 + 1)^{1/2}}{n^2}\left[1 - \frac{1}{n^2}\right] = \left(\frac{1}{\cos\theta} - \cos\theta\right)f \tag{3.36}$$

This is the relation Kohn et. al. [26] presented for the compensated cavity with $R_2 = \infty$ (1).

Simplifying 3.36 by setting

$$\frac{(n^2 + 1)^{1/2}}{n^2} \left[1 - \frac{1}{n^2}\right] = N \qquad (3.37$$

(hence N is a function of the index of refraction only)

gives

$$Nt = \left(\frac{1}{\cos\theta} - \cos\theta\right) f$$

This shows more clearly the trade-off made between cell thickness (t), and angle of incidence (θ) to yield the compensated cavity.

---

(1) Reference [26] actually stated

$$\frac{R_3}{2} \left(\frac{1}{\cos\theta} - \cos\theta\right) = t\left(\frac{n^2 + 1}{n^2}\right)^{1/2} \left[1 - \frac{1}{n^2}\right]$$

but $\left(\frac{n^2 + 1}{n^2}\right)^{1/2}$

instead of $\frac{(n^2 + 1)^{1/2}}{n^2}$ seems to be a printing error.

D. BEAM BEHAVIOUR IN THE COMPENSATED CAVITY

It was shown in section III. A. that, due to the threshold requirements and the limited available output power of present excitation sources, one has to achieve a certain spot size. The effects of the parameters of the compensated cavity (f, θ, t) on the beam area of the excitation beam will now be investigated.

1. Beam Radius and Location in the Empty Cavity

After reducing the Three Element system to an empty resonator (section III. B.) with mirrors R_1 and R_2^* (3-3), the diameter of the beam waist $2w_o$ (measured at the $1/e^2$ intensity points) is given by [31]:

$$w_o^4 = \left(\frac{\lambda}{\pi}\right)^2 \frac{d(R_1-d)(R_2^*-d)(R_1 + R_2^* - d)}{(R_1 + R_2^* - 2d)^2} \tag{3.39}$$

Using equations 3.1, 3, 6, 7, 10, and 3.11 this can be expressed as:

$$w_o^4 = \left(\frac{\lambda}{\pi}\right)^2 \frac{(R_1 + \delta - \delta_{max})(R_1 + \delta - \delta_{min})(\delta_{max} - \delta)(\delta - \delta_{min})}{(R_1 + 2\delta - \delta_{max} - \delta_{min})^2} \tag{3.40}$$

This expresses the beam width in terms of the adjustment measure δ.

If $R_1 >> 2S$ equation 3.40 reduces to

$$w_o^4 = \left(\frac{\lambda}{\pi}\right)^2 (\delta_{max} - \delta)(\delta - \delta_{min}) \tag{3.41}$$

which indicates that $w_o = 0$ at the limits of cavity stability.

In the center of the stability range

$$\delta = \frac{\delta_{max} + \delta_{min}}{2}$$

Equation 3.40 is evaluated as

$$w_{o\ center}^{4} = \left(\frac{\lambda}{\pi}\right)^{2} S^{2}\left[1 - \frac{S^{2}}{R_{1}^{2}}\right] \tag{3.42}$$

which under the above assumption, $R_1 >> 2S$, leaves

$$w_{o\ center}^{4} \sim \left(\frac{\lambda}{\pi}\right)^{2} S^{2} \tag{3.43}$$

which relates the beam waist to the stability factor.

The evaluation of the waist location (t_1, the distance from mirror R_1 to waist location) follows the same procedure as the waist radius. From Kogelnik and Li [31]:

$$t_1 = \frac{d(R_2^{*} - d)}{(R_1 + R_2^{*} - 2d)} \tag{3.44}$$

which can be rewritten as

$$t_1 = \frac{(R_1 + \delta - \delta_{max})(R_1 + \delta - \delta_{min})}{(R_1 + 2\delta - \delta_{max} - \delta_{min})} \tag{3.45}$$

If $R_1 >> 2S$ equation 3.45 reduces to

$$t_1 = R_1 \tag{3.46}$$

This shows that t_1 stays essentially fixed, when d_1 is adjusted through the stability range. In the center of the stability range

$$\delta = \frac{\delta_{max} + \delta_{min}}{2} \tag{3.47}$$

$$t_{1\ center} = R_1 - \frac{S^{2}}{R_1}$$

which, in the limits of the stability range (S=0), also reduces to

$$t_1 = R_1 \tag{3.48}$$

This locates the beam waist position.

Based on these investigations of the empty resonator, the effects of the tilt of mirror R and the insertion of the Brewster cell can now be considered.

2. Tilt of Mirror R

It was shown in section III. C. 3. that the stability range 2S could be considered essentially the same in the sagittal (X) and the tangential (Y) plane. This, together with equation 3.43, gives

$$w_x \sim w_y \sim w_o \tag{3.49}$$

in the center of the stability range.

The different waist locations are readily evaluated by equations 3.46 and 3.47 as

$$t_{1x} \sim t_{1y} \sim R_1 \tag{3.50}$$

3. Insertion of the Brewster Cell

It is assumed that:

(1) the waist location is inside the dye cell (necessary for dye laser operation)

(2) the cell windows and the dye are homogeneous material as far as the index of refraction (n) is concerned.

The wavelength inside the dye cell is

$$\lambda_r = \frac{\lambda}{n} \tag{3.51}$$

Recalling equations 3.22 and 3.23, it is necessary to construct the effective mirror (R_1) - to-waist spacing out of two parts [30]. These parts are the distance from mirror R_1 to the entrance of the cell, and the effective distance inside the cell

$$t_{1x} = t_{air} + \tau_x \frac{(n^2 + 1)^{1/2}}{n^2} \tag{3.52}$$

$$t_{1y} = t_{air} + \tau_y \frac{(n^2 + 1)^{1/2}}{n^4} \tag{3.53}$$

The distance τ is measured normal to the cell window as indicated in Figure 10.

If equation 3.50 is applied, τ_x is related to τ_y by

$$\tau_x \sim \frac{\tau_y}{n^2} \tag{3.54}$$

since t_{air} is the same in the sagittal and in the tangential plane.

Kogelnik et. al. [28] postulate a symmetrical configuration as a solution that should be very close to a practical optimum. This symmetrical configuration assumes that waists in the sagittal and in the tangential planes are equidistant from the center of the cell with

$$\tau_x + \tau_y = t \tag{3.55}$$

Combining 3.54 and 3.55 results in

$$\tau_x = \frac{t}{n^2 + 1} \tag{3.56}$$

$$\tau_y = \frac{t\, n^2}{n^2 + 1} \tag{3.57}$$

from which a compensation measure ($\Delta \tau$) is defined as

$$\Delta \tau \equiv \tau_y - \tau_x = \frac{t(n^2 - 1)}{n^2 + 1} \tag{3.58}$$

The general statement of the compensated cavity, achieved by getting the maximum overlap of the x and y- stability ranges, is modified by equation 3-58 which states that even with maximum compensation there remains a difference in the position of the stability ranges (i.e. complete overlap is not possible). For dye laser operation ($n \sim 1.4$) this difference is on the order of one-third of the cell thickness.

The light inside the cell propagates along the path Λ as indicated by Figure 10.

$$\Lambda = \frac{\tau}{\cos\Phi_n} = \frac{\tau(n^2 + 1)^{1/2}}{n} \tag{3.59}$$

where $\cos\Phi_n$ was evaluated with the help of Snell's law

$$\frac{\sin\Phi_B}{\sin\Phi_n} = n$$

and equation 3.21

$$\sin^2\Phi_B = \frac{n^2}{n^2 + 1}$$

Kogelnik and Li [31] expressed the expansion of a gaussian beam, a distance z away from the beamwaist, as

$$w(z) = w_o \left[1 + \left(\frac{\lambda z}{\pi w_o^2}\right)^2\right]^{1/2} \tag{3.60}$$

Assuming for simplicity that the beamwaist is located just inside of the entrance window of the dye cell and recalling that the beam diameter, when entering the cell, is changed under the laws of refraction to

$$w_{x\ cell} = w_x = w_o \tag{3.61}$$

$$w_{y\ cell} = \frac{\cos\Phi_n}{\cos\Phi_B} w_y = n\, w_o \tag{3.62}$$

The expansions of the beam radii as a function of the propagation distance along the beam axis are given by

$$w_{x\ cell}(\Lambda) = w_o \left[1 + \left(\frac{\lambda\, \Lambda}{\Pi n\, w_o^2}\right)^2\right]^{1/2} \tag{3.63}$$

$$w_{y\ cell}(\Lambda) = n\, w_o \left[1 + \left(\frac{\lambda\, \Lambda}{\Pi n^3\, w_o^2}\right)^2\right]^{1/2} \tag{3.64}$$

If one now defines the cross sectional beam area [28]

$$A \equiv \Pi\, w_{x\ cell}\, w_{y\ cell} \tag{3.65}$$

and replaces the parameter Λ by the variables $(\Lambda - \Lambda_x)$ and $(\Lambda - \Lambda_y)$ to cover different waist locations Λ_x and Λ_y [28], the cross sectional beam area can be written as

$$A(\Lambda) = \Pi n\, w_o^2 \left[1 + \left(\frac{\lambda}{\Pi n\, w_o^2}\right)^2 (\Lambda - \Lambda_x)^2\right]^{1/2} \left[1 + \left(\frac{\lambda}{\Pi n^3 w_o^2}\right)^2 (\Lambda - \Lambda_y)^2\right]^{1/2} \tag{3.66}$$

In the symmetrical configuration

$$\Lambda_x = \frac{t}{n(n^2 - 1)^{1/2}} \tag{3.67}$$

$$\Lambda_y = \frac{tn}{(n^2 + 1)^{1/2}} \tag{3.68}$$

Now equation 3.66 is the desired relationship, since it relates the beam area A to the cell thickness t by equations 3.67 and 3.68 and to the focal length f by equations 3.13 and 3.43. The latter two can be combined to give

$$2S \sim \frac{f^2}{d_2} \sim \frac{2\Pi w_o^2}{\lambda} \tag{3.69}$$

where $\frac{2\Pi w_o^2}{\lambda}$ is known as the confocal parameter.

E. CAVITY DESIGN DATA

Assume the following cavity design data:

$R_1 = 5\times10^{-2}$ m

$R = 2f = 10\times10^{-2}$ m

$R_2 = \infty$

$d_1 = 10\times10^{-2}$ m

$d_2 = 2.0$ m

$t = 1.5\times10^{-3}$ m

$\lambda = 0.488$ μm

$n = 1.333$ [24]

The evaluation of equation 3.66, assuming the symmetrical configuration, for different propagation distances Λ is given in TABLE III.

TABLE III

Evaluation of Equation 3.66

$\Lambda(x10^{-3})m$	$A(x10^{-10})m^2$
0.000	6.273
0.300	2.773
0.633	3.205
0.900	1.600
1.200	3.205
1.500	5.211

Hence $\Lambda = 0.9x10^{-3}$ m gives the smallest crossectional beam area A.

The single line (λ = 0.488 μm) output power for a "Control Laser" Model 902 as excitation source was measured ad 1.2W for a 2 mm (at $1/e^2$ intensity points) beam diameter. This laser would yield an excitation power density at the minimum cross sectional beam area ($A=1.6x10^{-10}$ m^2) of 750 KW/cm^2. That would lie well above the stated threshold condition of 100 KW/cm^2. To indicate the trade-offs between beam area A, focal length f, and cell thickness t, first focal length and then the cell thickness are varied. The results of these calculations are indicated in TABLE IV (variable focal length) and TABLE V (variable cell thickness).

TABLE IV

Evaluation of Equation 3.66

(Focal length f is varied, other data as in original listing)

	$f=3 \times 10^{-2}$ m	$f=10 \times 10^{-2}$ m
Λ ($\times 10^{-3}$) m	A ($\times 10^{-10}$) m^2	A ($\times 10^{-10}$) m^2
0.000	15.274	11.889
0.300	6.676	11.158
0.633	3.042	10.744
0.900	2.521	10.744
1.200	3.344	3.200
1.500	7.061	11.719

TABLE V

Evaluation of Equation 3.66

(Cell thickness t is varied, other data as in original listing)

	$t = 0.5 \times 10^{-3}$ m	$t = 10 \times 10^{-3}$ m
Λ ($\times 10^{-3}$) m	A ($\times 10^{-10}$) m^2	A ($\times 10^{-10}$) m^2
0.000	3.264	246.754
0.225	2.707	
0.400	2.829	
0.900	5.417	
1.200	8.474	
1.500	12.712	
2.000		104.482
4.500		11.436
6.000		23.086
8.000		19.952
10.000		81.099

The comparison of TABLES III, IV, and V indicates that the original design data gave the highest excitation power of the cases considered.

Using these data to evaluate equation 3.38, yields

$$\theta = 6^{o}\ 21'$$

With the evaluated angle of incidence θ and the previous data the dye laser system is completely specified.

IV. EXPERIMENTAL SET UP AND PROCEDURE

A. RESONATOR DATA

The experimental set up is shown in Figure 11 which is related to Figure 8 since all parameters given in that figure remain valid for Figure 11. The excitation (Argon) laser is inserted in the long leg of the cavity with its front end F (F ≡ laser front, E ≡ laser end) pointing toward the short part of the cavity.

The acutal parameters were chosen as indicated in section III. E.. For the excitation wavelength of 0.488 μm the dye lasing was expected at 0.565 μm. This determined the coatings for the mirrors R_1 , R , and R_2 . Mirrors R_1 and R (R_1=5cm, R=10cm) were designed as high reflectors (reflectivity > 99.5%) in the region from 0.480 μm to 0.580 μm; see Figure 12. Mirror R_2 (R_2= ∞) which is the output mirror for the dye laser had a high reflectivity (> 99.5%) from 0.480 μm to 0.520 μm. The reflectivity for longer wavelengths slowly decreased to reach a 3.5% transmission at the expected lasing wavelength of 0.565 μm; see Figure 13. The cavity lengths d_1 and d_2 were chosen as 10 cm and 200 cm respectively. The 10^{-4} M solution of Rhodamine 6G (n=1.333) in water with 4% Ammonyx LO (triplet quencher, provided by Onyx Chemical Company, Jersey City, New Jersey) was pumped through the dye cell with thickness t=1.5 mm as indicated in Figure 11.

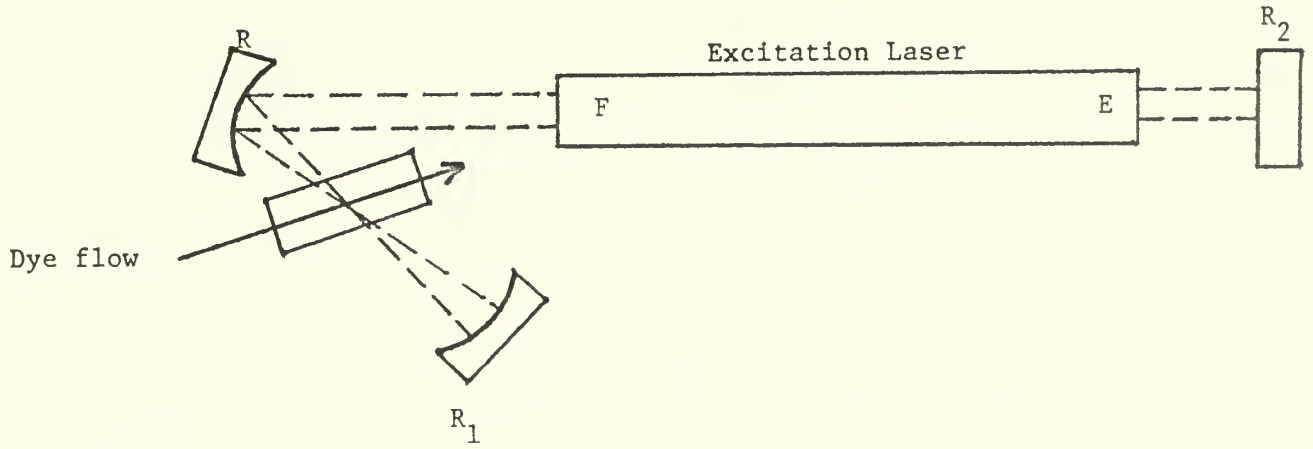

Fig. 11: Experimental Set up

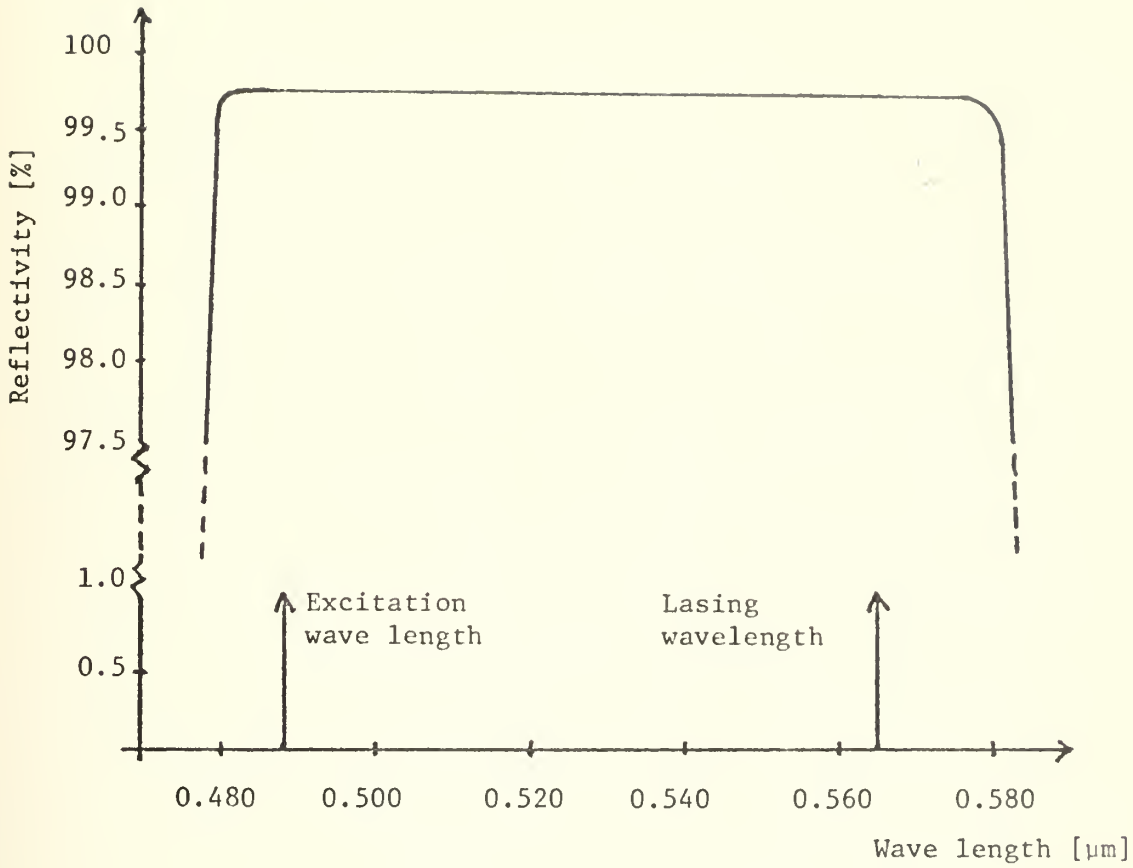

Fig. 12: Reflectivity of Mirrors R_1 and R

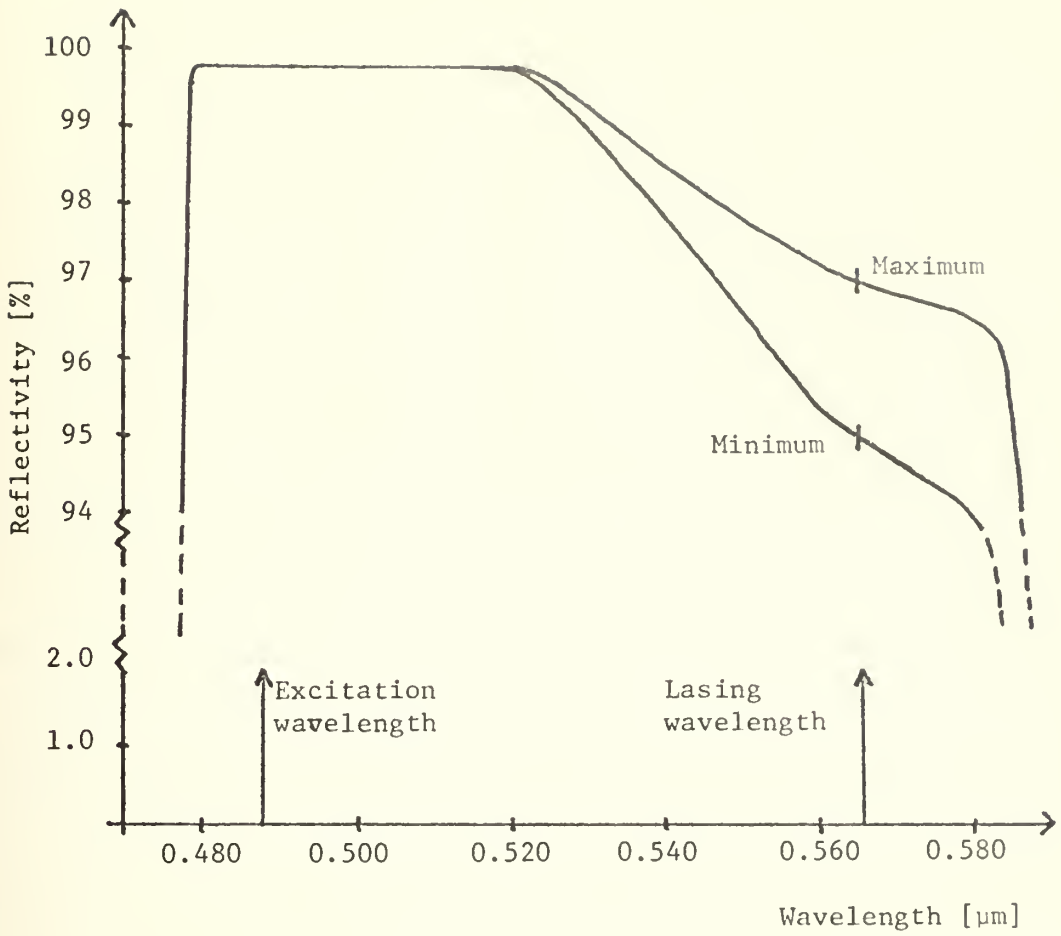

Fig. 13: Reflectivity of Mirror R_2. Maximum and Minimum Values of Reflectivity at the lasing wavelength are indicated

B. PROCEDURE

Since excitation and dye laser have to use the same cavity the excitation laser was put in the long leg of the cavity. The task was to align mirrors R_1 , R , and R_2 to form the laser resonator.

The first try align all three mirrors failed.

The next attempt was to align mirror R_2 with an argon laser output mirror inserted at end F to form a resonator for the excitation source only. This alignment was achieved relatively easy. The folded part of the cavity, mirrors R_1 and R, were now adjusted into rough alignment. The expected very tight focus inside the dye cell could be observed. Removal of mirror F and attempts to achieve lasing action in the folded cavity failed. This proved that the folded part of the cavity was not aligned with the flat mirror R_2. Efforts to align the folded part of the cavity proved fruitless. The fact that two mirrors had to be adjusted made alignment quite difficult.

To overcome this difficulty the excitation laser was turned around in order to align the folded part of the resonator first. The flat mirror R_2 would be adjusted after the mirror F was removed. This seemed to be more reasonable since the adjustment of a single mirror introduced only minor difficulties.

The experiment was stopped during this set up since the excitation laser broke down and failed to produce a usable discharge.

The experiments have shown that even in this configuration the alignment of the cavity is the critical step in achieving cw dye laser action. Rigid, very fine adjustable mounts for the mirrors and the cell as well as a vibration-free environment are necessary.

BIBLIOGRAPHY

1. Maiman, T. H., "Simulated Optical Radiation in Ruby", Nature, v. 187, p. 493-494, 6 August 1960

2. Sorokin, P. P., Stevenson, M. J., "Stimulated Infrared Emission from Trivalent Uranium", Phys. Rev. Letters, v. 5, no. 12, p. 557-559, 15 December 1960

3. Yariv, A., Gordon, J. P., "The Laser", Proc. IEEE, v. 51, no. 1, p. 4-29, January 1963

4. Brock, E. G., Czavinsky, P., Hormats, E., Nedderman, H. C., Stirpe, D., Unterleitner, F., "Coherent Stimulated Emission form Organic Molecular Crystals", J. Chem. Phys., v. 35 no. 2, p. 759-760, August 1961

5. Rautian, S. G., Sobel'man, I. I., "Remarks on Negative Absorption", Optics and Spectroscopy, v. 10, no. 1, p. 65-66, January 1961

6. Morantz, D. J., White, B. C., Wright, A. J. C., "Stimulated Light Emission by Optical Pumping and by Energy Transfer in Organic Molecules", Phys. Rev. Letters, v. 8, no. 1, p. 23-25, 1 January 1962

7. Lempicki, A., Samelson, H., "Stimulated Processes in Organic Compounds", Appl. Phys. Letters, v. 2, no. 8, p. 159-161, 15 April 1963

8. Stockman, D. L., Mallory, W. R., Tittel, K. F., "Stimulated Emission in Aromatic Organic Compounds", Proc. IEEE, v. 52, no. 3, p. 318-319, March 1964

9. Sorokin, P. P., Lankard, J. R., "Stimulated Emission Observed from an Organic Dye Chloro-aluminium Phthalocyanine", IBM J. Res. Develop., v. 10, p. 162-163, March 1966

10. Sorokin, P. P., Lankard, J. R., "Flashlamp Excitation of Organic Dye Lasers: A Short Communication", IBM J. Res. Develop., v. 11, p. 148, March 1967

11. Peterson, O. G., Tuccio, S. A., Snavely, B. B., "CW Operation of an Organic Dye Solution Laser", Appl. Phys. Letters, v. 17, no. 6, p. 245-247, 15 September 1970

12. Shank, C. V., Dienes, A., Trozzolo, A. M., Myer, J. A., "Near Uv to Yellow Tunable Laser Emission from an Organic Dye", Appl. Phys. Letters, v. 16, no. 10, p. 405-407, 15 May 1970

13. Shank, C. V., Bjorkholm, J. E., Kogelnik, H., "Tunable Distributed-Feedback Dye Laser", Appl. Phys. Letters, v. 18, no. 9, p. 395-396, 1 May 1971

14. Dienes, A., Ippen, E. P., Shank, C. V., "High Efficiency Tunable CW Dye Laser", IEEE J. of Quant. Electron., v. QE-8, no. 3, p. 388, March 1972

15. Bass, M., Deutsch, T. F., and Weber, M. J., Dye Lasers, in Lasers, edited by Levine, A. K. and DeMaria, A. J., v. 3, ch. 3, p. 272-274 and p. 278-285, Marcel Dekker, 1971

16. Beiser, A., Perspectives of Modern Physics, p. 342, McGraw-Hill, 1969

17. Snavely, B. B., "Flashlamp-Excited Organic Dye Lasers", Proc. IEEE, v. 57, no. 8, p. 1374-1390, 8 August 1969

18. Weber, M. J., Bass, M., "Frequency- and Time-Dependent Gain Characteristic of Dye Lasers", IEEE J. of Quant. Electron., v. QE-5, p. 175-188, April 1969

19. Lower, S. K., El-Sayed, M. A., "The Triplet State and Molecular Electronic Process in Organic Molecules", Chem. Rev., v. 66, no. 2, p. 199-241, April 1966

20. Snavely, B. B., Peterson, O. G., "Experimental Measurement of the Critical Population Inversion for Dye Solution Laser", IEEE J. of Quant. Electron., v. QE-4, no. 10, p. 540-545, October 1968

21. Bennet, R. G., McCartin, P. J., "Radiationless Deactivation of the Fluorescent State of Substituted Anthracenes", J. Chem. Phys., v. 44, no. 5, p. 1969-1972, 1 March 1966

22. Windsor, M. W., Novak, J. R., "Studies of Radiationless Transitions in Coronene using Nanosecond Laser Photolysis and Spectroscopy", Molecular Luminescence, (An International Conference), W. A. Benjamin Inc., 1969

23. Snavely, B. B., Schäfer, F. P., "Feasibility of cw Operation of Dye-Lasers", Phys. Letters, v. 28A, no. 11, p. 728-729, 10 March 1969

24. Tuccio, S. A., Strome, Jr., F. C., "Design and Operation of a Tunable Continuous Dye Laser", Appl. Opt., v. 11, no. 1, p. 64-73, January 1972

25. Maydan, D., "Fast Modulator for Extraction of Internal Laser Power", J. Appl. Phys., v. 41, no. 4, p. 1552-1559, 15 March 1970

26. Kohn, R. L., Shank, C. V., Ippen, E. P., Dienes, A., "An Intracavity-Pumped CW Dye Laser", Opt. Comm., v. 3, no. 3, p. 172-178, May 1971

27. Kogelnik, H., "Imaging of Optical Modes - Resonators with Internal Lenses", Bell Syst. Tech. J., v. 44, p. 455-594, March 1965

28. Kogelnik, H., Dienes, A., Ippen, E. P., Shank, C. V., "Astigmatically Compensated Cavities for CW Dye Lasers", IEEE J. of Quant. Electron., v. QE-8, no. 3, March 1972

29. Jenkins, F. A. and White, H. E., Fundamentals of Optics, 3rd., p. 149, McGraw-Hill, 1957

30. Hanna, D. C., "Astigmatic Gaussian Beams Produced by Axially Asymmetric Laser Cavities", IEEE J. of Quant. Electron., v. QE-5, no. 10, p. 483-488, October 1969

31. Kogelnik, H., Li, T., "Laser Beams and Resonators", Appl. Opt., v. 5, no. 10, p. 1550-1567, October 1966

INITIAL DISTRIBUTION LIST

		No. Copies
1.	Defense Documentation Center Cameron Station Alexandria, Virginia 22314	2
2.	Library, Code 0212 Naval Postgraduate School Monterey, California 93940	2
3.	Asst Professor J. P. Powers Code 52Po Naval Postgraduate School Monterey, California	5
4.	LT Karl-Heinz F. Kelle 2 Hamburg 26 Dimpfelweg 2, bei Hundertmark GERMANY	1
5.	Marineamt, Inspection der Offz./UOFFz. AusbM. 294 Wilhelmshaven GERMANY	1
6.	DOKZENT Bw-See 53 Bonn Friedrich-Ebert Allee 34 GERMANY	1

DOCUMENT CONTROL DATA - R & D

(Security classification of title, body of abstract and indexing annotation must be entered when the overall report is classified)

1. ORIGINATING ACTIVITY *(Corporate author)*
Naval Postgraduate School
Monterey, California 93940

2a. REPORT SECURITY CLASSIFICATION
Unclassified

2b. GROUP

3 REPORT TITLE

Design and Construction of a CW Dye Laser

4. DESCRIPTIVE NOTES *(Type of report and inclusive dates)*

5. AUTHOR(S) *(First name, middle initial, last name)*
Karl-Heinz Friedrich Kelle
Lieutenant, Federal German Navy

6. REPORT DATE
June 1972

7a. TOTAL NO. OF PAGES
57

7b. NO. OF REFS
31

8a. CONTRACT OR GRANT NO.

b. PROJECT NO.

c.

d.

9a. ORIGINATOR'S REPORT NUMBER(S)

9b. OTHER REPORT NO(S) *(Any other numbers that may be assigned this report)*

10. DISTRIBUTION STATEMENT

Approved for public release; distribution unlimited.

11. SUPPLEMENTARY NOTES

12. SPONSORING MILITARY ACTIVITY

Naval Postgraduate School
Monterey, California 93940

13. ABSTRACT

The properties of organic dyes as well as the lasing process of organic dye lasers are investigated to form the basis for the design of a cw dye laser. Different dye laser systems are compared with regard to stability, utility, and construction characteristics. A folded three mirror resonator with an inserted dye cell at the Brewster angle is chosen and analysed. The astigmatic effects introduced by the tilted mirror can be offset by those from the dye cell to yield a compensated cavity. The trade-offs and limitations given by the cell thickness, the angle of incidence, and the focal length of the center mirror are discussed. Finally, experimental data and procedures are given.

DD FORM 1 NOV 65 1473 (PAGE 1)
S/N 0101-807-6811

A-31408

KEY WORDS	LINK A		LINK B		LINK C	
	ROLE	WT	ROLE	WT	ROLE	WT
Organic Dye						
Energy Level						
Lasing Process						
Population Inversion						
Internal Conversion						
Inter System Crossing						
Compensated Cavity						
Astigmatic Effects						
Dye Cell						

Thesis 141371
K2552 Kelle
c.1 Design and construc-
tion of a cw dye laser.